



# Experimental investigation of fatigue strength of out-of-plane gusset welded joints under variable amplitude plate bending loading in long life region

Yuki Banno<sup>1</sup> · Koji Kinoshita<sup>1</sup>

Received: 25 October 2021 / Accepted: 27 April 2022 / Published online: 6 June 2022  
© International Institute of Welding 2022

## Abstract

This study investigated fatigue strength of out-of-plane gusset welded joints under variable amplitude plate bending loading in a long life region. First, constant amplitude stress fatigue tests using a plate bending fatigue test machine were previously carried out under  $R=0.0$ , around 0.5, and  $-1$ . Its fatigue limit (constant amplitude fatigue limit (CAFL)) was assumed from the minimum stress ranges in which fatigue failure occurred and was approximately 51, 40, and 45 MPa, which tended to depend on the stress ratio. Thereafter, a loading system for the machine was originally developed to handle variable amplitude stress. The system's accuracy was verified by a ratio of output versus input data and improved up to around 90% by slightly modifying applied loading conditions. Then, variable amplitude stress fatigue tests were carried out using the developed system under several magnitudes of variable stress ranges determined based on the CAFL. From the results, fatigue crack initiation and propagation occurred when any of the stress components exceeds the CAFL, despite the equivalent stress range being lower than it, and damage accumulation could be evaluated using the modified Miner's rule. In contrast, when none of the stress components exceeds the CAFL, fatigue crack initiation was not observed even after 500 million cycles.

**Keywords** Variable amplitude loading · Constant amplitude loading · Long life region · Out-of-plane gusset welded joints · Plate bending fatigue test

## 1 Introduction

It is well known that structure members in steel bridges are subjected to a large number of variable amplitude stress during their service lives [1–3]. An actual stress measurement shows that the majority of variable stress ranges is distributed in lower stress side of a recorded histogram [4]. Even though the stress ranges are biased toward the lower stress side, accumulation of fatigue damage on welded joints might be caused, resulting in crack initiation and propagation. It is thus of major importance to investigate fatigue behavior of

welded joints under variable amplitude stress including low stress ranges, i.e., in long life region.

Already, numerous studies on fatigue strength under variable amplitude loading in welded joints have been performed. However, its fatigue strength in the long life region has not been fully evaluated. The reason for this is that the experimental data in the long life region, particularly  $N > 10 \times 10^6$  cycles are very limited [5–7], since the fatigue tests are expensive and very time-consuming. Instead of experimental tests, several studies have investigated such fatigue behaviors so far numerically [8–11]. For instance, Miki et al. [9] estimated fatigue strengths and fatigue limits of various welded joints under variable amplitude loading in the long life region by numerical simulation applying a relationship between crack growth characteristics and the linear cumulative damage conception. Mori et al. [10] proposed a procedure to predict fatigue life under variable amplitude stress in the long life region by using fatigue crack propagation analysis.

Figure 1 shows format of fatigue design for variable amplitude loading used in several design codes. In the design

---

Recommended for publication by Commission XIII - Fatigue of Welded Components and Structures.

---

✉ Koji Kinoshita  
kinosita@gifu-u.ac.jp  
Yuki Banno  
banno@gifu-u.ac.jp

<sup>1</sup> Gifu University, Gifu, Japan

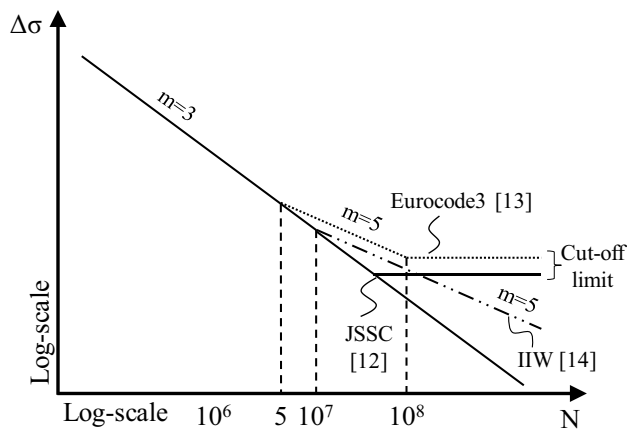


**Fig. 1** Format of fatigue design for variable amplitude loading used in several design codes

code of JSSC (Japanese Society of Structural Construction) [12], either the modified Miner's rule or it considering cutoff limit is employed. On the other hand, in the design code of Eurocode 3 [13], the curve's gradient is changed from  $m=3$  to  $m=5$  within the region of  $5 \times 10^6 < N < 10 \times 10^7$  cycles, and cutoff limit is adopted in the region of  $N > 10 \times 10^7$  cycles. In the design code of IIW (The International Institute of Welding) [14], it adopts not a cutoff limit but a change of curve's gradient, and its gradient is  $m=5$  in the region of  $N > 10 \times 10^6$  cycles. Even in these design codes, transition points and with or without cutoff limit are different on a fatigue strength evaluation under variable amplitude stress in the long life region due to scarce experimental data. Therefore, an efficient fatigue test system for variable amplitude loadings with superior features, such as low running cost and fast test speed, is strongly aspired to be developed.

A plate bending fatigue test machine was recently developed [15] and has been widely used in Japan [16–18]. An outstanding advantage for the plate bending fatigue test machine is a loading speed. It can run a fatigue test with

around 20-Hz frequency. With its faster loading frequency operation, one can achieve to obtain the fatigue test data of over 10 million cycles at low stress levels in a relatively short period. In a previous study [19], the fatigue strength of out-of-plane gusset welded joints under constant amplitude loading in the long life region of more than 10 million cycles by using the machine has been studied. Therefore, a further development of a loading system, which enables to study variable amplitude stress, for the machine is needed.

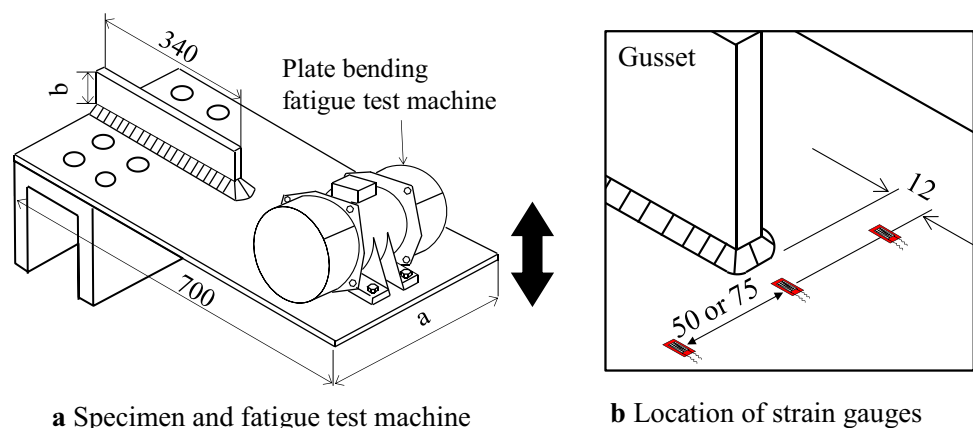
This study investigated fatigue strength of out-of-plane gusset welded joints under variable amplitude plate bending loading in the long life region. First, in order to obtain the constant amplitude fatigue limit, namely CAFL, constant amplitude stress fatigue tests were carried out using the plate bending fatigue test machine in the co-authors' previous study [20]. Thereafter, to handle variable amplitude stress, a loading system for the machine was originally developed and the system's accuracy was verified in the authors' previous study [21]. Then, variable amplitude stress fatigue tests were carried out using the developed system under several magnitudes of variable stress ranges determined based on the CAFL. The test results were discussed in terms of fatigue strength, fatigue life, and damage accumulation.

## 2 Outline of plate bending fatigue test setup

### 2.1 Plate bending fatigue test

Figure 2 shows a fatigue test setup of plate bending developed by Yamada et al. [15]. The specimen geometry of out-of-plane gusset welded joints is given in Fig. 2a. The specimen is fixed to a jig like cantilever beam. Bending forces are applied to the specimen through the machine equipping with an eccentric mass inside. The machine produces an excitation force due to vibration of the mass. Stress ranges at interest location must be monitored by strain gauges because they

**Fig. 2** Setup of fatigue test machine and location of strain gauges (unit: mm)



depend on magnitudes of the excitation force derived from a rotation speed of the mass. Location of strain gauges is shown in Fig. 2b. In this study, with reference to the previous studies [17, 19, 22], strain gauges were attached 12 mm away from the weld toe and 50 or 75 mm away from the center of the width of the specimen. The 12-mm location was used for monitoring fatigue crack initiation, and the 50- or 75-mm location was used for calculation of nominal stress range. An inverter installed in the machine controls the rotation speed of the mass, and its maximum value is approximately 20 Hz. The speed coincides with loading frequency of fatigue tests; i.e., one can run a test with 20 Hz under constant amplitude loadings when the inverter is set to 20 Hz.

To detect fatigue crack initiation and propagation, a copper wire with a diameter of 0.05 mm was glued in the vicinity of/around the weld toe. Figure 3 shows the locations of the glued copper wire [15] and definition of fatigue lives in accordance with fatigue crack lengths. When fatigue cracks are initiated from the weld toe and propagate along the weld toe, these cracks are defined as  $N_{toe}$  and  $N_b$ , respectively. Fatigue crack separates from the weld toe and propagates to the base metal. When the crack length becomes 10 or 20 mm away from the weld toe, the crack is defined as  $N_{10}$  or  $N_{20}$ , respectively. At  $N_{20}$ , fatigue crack propagates to more than 80% of plate thickness in a depth direction [19]; thus, the final failure of the specimen is defined as  $N_{20}$ . In [20], fatigue cracks were captured at fatigue crack length of 30 mm away from the weld toe,

which was defined as  $N_{30}$ . The glued copper wire is cut by either fatigue crack initiation or propagation, and the plate bending fatigue test machine automatically stops. At this moment, the number of cycles is recorded. To ensure the existence of fatigue cracks, magnetic particle testing is performed as well.

### 2.2 Out-of-plane gusset welded joints specimen

The specimens are made of 490-MPa class steels, Japan Industrial Standard-SM490. The mechanical properties and chemical compositions are given in Table 1. The specimens have almost the same geometry, but some have the different main plate widths and gusset heights as shown in Table 1 and Fig. 2a. Ones that have 300 and 100 mm for pilot test, 300 and 300 mm for constant amplitude stress fatigue tests, and 200 and 100 mm for variable amplitude stress fatigue tests were used respectively. To avoid fatigue cracks from the weld root area, full-penetration welding was applied up to 50 mm from the weld toe. In the design code of JSSC, the classification reference of the out-of-plane gusset welded detail is categorized into G class (50 MPa), corresponding to 2 million fatigue strength. The fatigue limit and cutoff limit are 32 and 15 MPa for constant amplitude and variable amplitude loading, respectively.

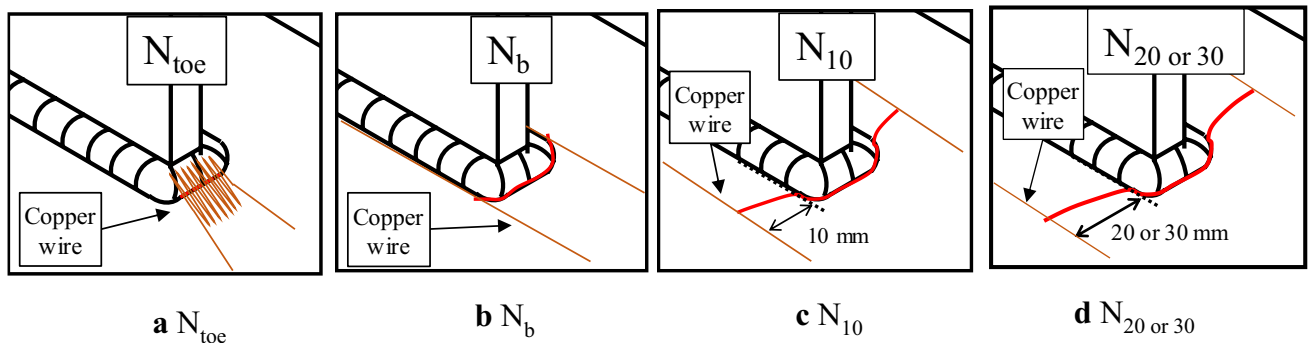


Fig. 3 Definition of fatigue lives in accordance with fatigue crack lengths

Table 1 Mechanical properties and chemical compositions and detail of plate width and gusset height

Type of steel	Yield strength (MPa)	Tensile strength (MPa)	Elongation (%)	Chemical composition (%)					Plate width a (mm)	Gusset height b (mm)	Ref
				C	Si	Mn	P	S			
SM490	-	-	-	×100					300	100	-
	395	559	23	16	34	143	13	5	300	300	[20]
	378	546	26	16	43	144	14	3	200	100	-

### 3 Fatigue test under constant amplitude loading [20]

#### 3.1 Test condition

To obtain the constant amplitude fatigue limit (CAFL), the constant amplitude stress fatigue tests have been carried out in the co-authors' previous study. A total of 12 specimens were tested at stress ratios of  $R=0.0$ ,  $-1$ , and around  $0.5$ . The fatigue tests were continued until a fatigue crack length reached up to either  $N_{20}$  or  $N_{30}$ . At each stage on the crack lengths, beach mark tests were carried out. A nominal stress range was increased when no crack was recognized in more than 20 million cycles.

#### 3.2 Test results

Figure 4 shows the fatigue test results. The detailed information such as stress range, stress ratio, and the number of cycles required for reaching each fatigue life on fatigue crack lengths are given in Table 2. The specimens are named using the initial letters of constant amplitude loading and numbered, e.g., CA1. In addition to the fatigue test results in the present study, this figure indicates fatigue test results that were carried out under  $R = -1$  using the same specimen geometry as the present study by Yamada et al. [15]. Also indicated in this figure are the fatigue design curves for constant amplitude stress given by the design code of JSSC. Arrow marks mean that there is no fatigue crack at the weld toe.

From Fig. 4, it can be seen that all specimens in which fatigue failures occurred are plotted along the curve of JSSC-F class. Within the specimens, the results are arranged by the stress ratio in order to obtain the CAFL. It is defined as a minimum stress range in which fatigue failures occurred. As results, the CAFL is 51 MPa under  $R=0.0$ , the one is 40 MPa under around  $R=0.5$ , and the one is 53 MPa under  $R = -1$ . Meanwhile, referring to the Yamada et al.'s result [15], fatigue crack of  $N_{toe}$  was observed at equivalent stress range 45 MPa, and then fatigue crack reached  $N_{10}$  at equivalent stress range 51 MPa. Hence, the CAFL is determined as 45 MPa under  $R = -1$ . As a result, a different CAFL is observed depending on the stress ratio. Previous studies showed that either tensile residual stresses [23] or compressive residual stresses [24] are present at the weld toe of out-of-plane gusset welds. Occurrence of compressive residual stress around the weld toe is presumed to be due to the deformation of the base plate toward the gusset plate during cooling after welding because a gusset is welded on one side of a base plate (see Fig. 2a). Although the residual stress states at the welds of constant amplitude stress fatigue test specimens were not exactly confirmed, it is probable that the stress ratio affects their stress states at the welds. After fatigue tests, to confirm whether a small fatigue crack is initiated from the weld toe, the run-out specimens were cut out. Their cross-sections were observed using a microscope whose magnification was approximately  $\times 200$ . The observation results showed that there was no visible fatigue crack. Thus, it is found from the experimental results that the CAFL tended to depend on the stress ratio, resulting in 51 MPa under  $R=0.0$ , 40 MPa under  $R=0.5$ , and 45 MPa under  $R = -1$ , respectively.

Fig. 4 Fatigue test results under constant amplitude loading [15, 20]

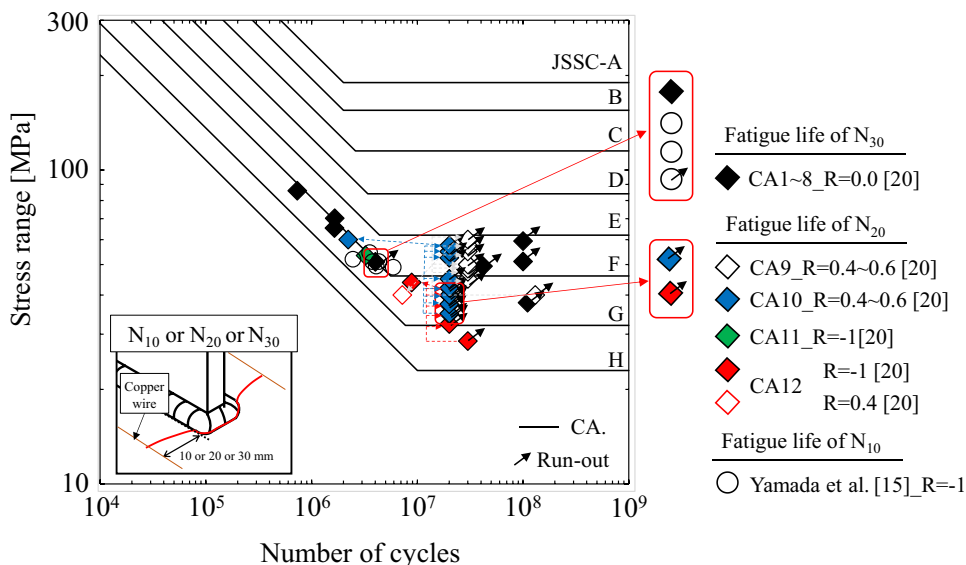


**Table 2** List of specimens for constant amplitude stress fatigue test [20]

Specimen	Stress range [MPa]	Stress ratio, R	Number of cycles required for reaching each fatigue life					Crack initiation
			N <sub>toe</sub>	N <sub>b</sub>	N <sub>10</sub>	N <sub>20</sub>	N <sub>30</sub>	
CA1	37.8	0.0	110000000					-
CA2	49.4		41700000					-
CA3	51.1		100000000					-
CA4	51.0		-	-	-	-	4000000	Weld toe
CA5	59.4		100000000					-
CA6	65.3		-	-	-	-	1650000	Weld toe
CA7	70.2		-	-	-	-	1650000	Weld toe
CA8	85.9		-	-	-	-	730000	Weld toe
CA9	28.5	0.6	30000000					-
	32.3	0.5	20000000					
	34.7	0.5	20000000					
	37.1	0.5	20000000					
	39.8	0.4	20000000					
	42.0	0.4	20000000					
	43.8	0.4	1286600	3356900	6154800	8829700	-	Weld toe
CA10	34.9	0.4	20000000					-
	37.4	0.4	20000000					
	39.9	0.4	20000000					
	42.1	0.4	20000000					
	45.0	0.5	60000000					
	47.8	0.6	30000000					
	50.0	0.6	30000000					
	52.5	0.6	20000000					
	55.0	0.6	20000000					
	57.5	0.6	20000000					
60.0	0.6	2098000	-	2137500	2219600	-	Weld toe	
CA11	53.4	-1	955200	1912200	2676400	3231100	-	Weld toe
CA12	40.0		130000000					-
	45.0		30000000					
	47.4		30000000					
	48.5		30000000					
	50.0		30000000					
	55.0		30000000					
	57.5		30000000					
	60.0		30000000					
40.0	0.4		1114000	2912100	4865300	7184200	-	Weld toe

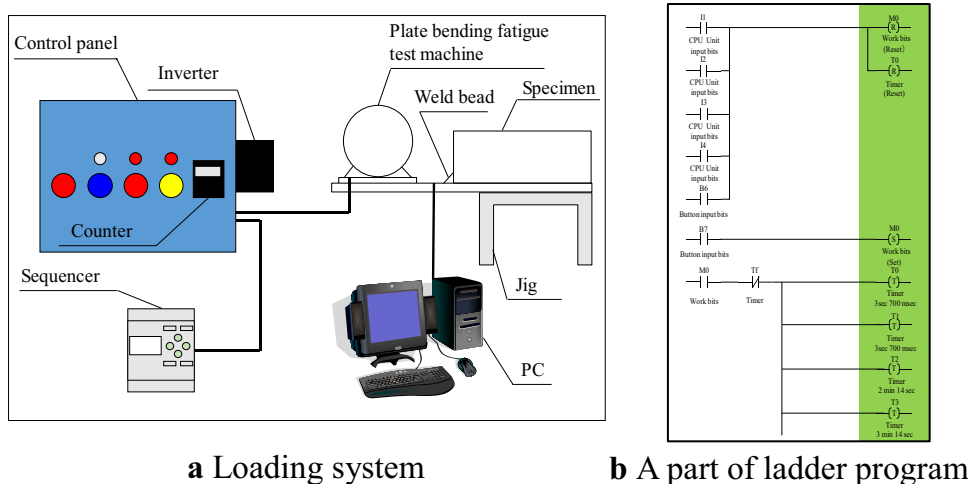
## 4 Fatigue test under variable amplitude loading

### 4.1 Developed variable amplitude loading system

Figure 5 shows a variable amplitude stress fatigue test system developed for the plate bending fatigue test machine. A

sequencer allows to apply the variable loading on the specimen. The sequencer, Omron Zen 10C1AR-A-V2, is additionally incorporated into the machine as shown in Fig. 5a, and it is capable of giving an external automatic control to the inverter. A ladder program is inputted to the sequencer, consisting of an on-off control circuit based on a set timer. A part of ladder program is shown in Fig. 5b. By using the

**Fig. 5** Developed variable amplitude stress fatigue test system



inverter controlled by the sequencer in accordance with the ladder program, one can achieve a variable amplitude stress fatigue test with plural loading frequencies which are determined in advance. Since the inverter can assign up to different 15 steps for loading frequencies, a fatigue test with maximum 15 steps variable amplitude stress is feasible.

**4.1.1 Frequency distribution and loading sequence**

A previous study [2] collected numerous stress histories and/or histograms that were recorded on various types of highway bridges by strain gauges. These stress ranges were normalized with respect to each maximum stress range, while low-stress ranges below 25% of maximum stress range were omitted. After that, the cumulative frequency distribution curve was computed by the least squares function. The cumulative frequency distribution can be expressed as follows:

$$f(x) = -12.0 \cdot (x - 1.0)^3 + 0.07 \tag{1}$$

where  $x = \sigma / \sigma_{max}$  ( $0.25 \leq x \leq 1.0$ ) is the normalized stress range. Note that the area sum between  $x=0.25$  and  $x=1.0$  is equal to 1 in this function. The calculated average probability density is shown in Fig. 6, corresponding to a histogram of 15 bars. In a previous study [25], a 15-block loading sequence which is derived from the histogram rearranged as a function of random number table was used to carry out the variable amplitude stress fatigue test. Figure 7 shows the 15-block loading sequence. It was used in this study as well.

**4.1.2 Determination of test conditions and pilot test**

A previous study [15] stated that the resonance between the specimen and the machine generated by increase of applied stress range accidentally should be avoided. Thus,

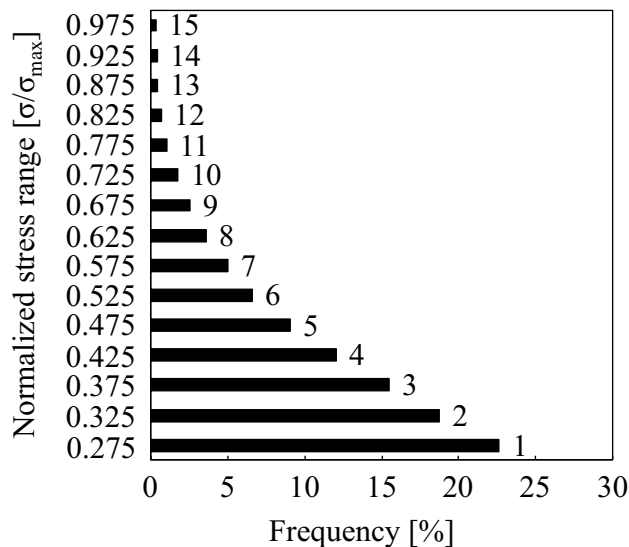


**Fig. 6** Relationship between normalized stress range and frequency distribution [2]

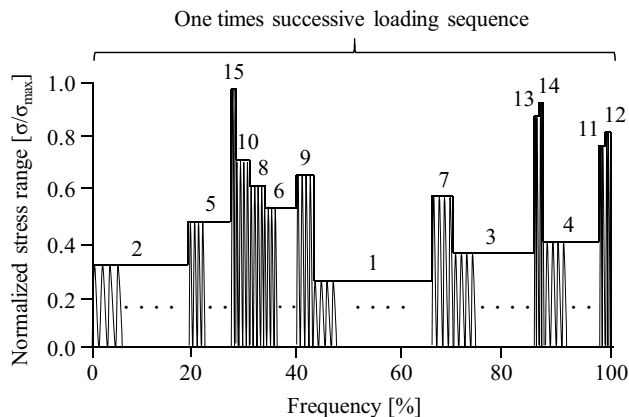


**Fig. 7** 15-block loading sequence [25]

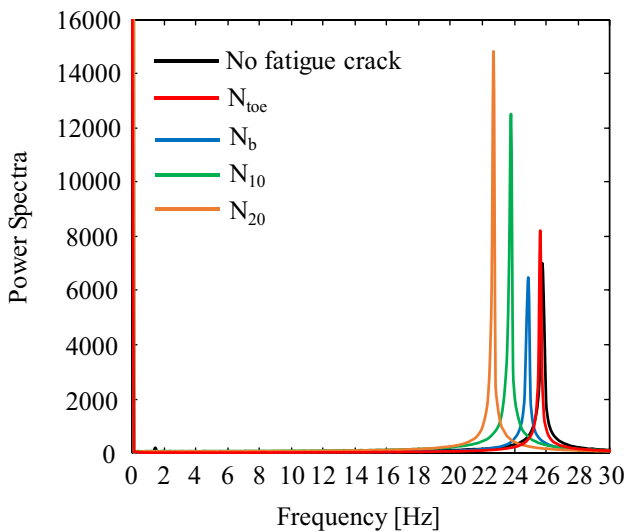


**Fig. 8** Relationship between power spectra and natural frequency

a natural frequency of the specimen was measured before a pilot test. Figure 8 shows the results of the natural frequency measurement. Relationships between power spectra and the natural frequency at different stages on fatigue lives in accordance with fatigue crack lengths are shown in this figure. The relationships were obtained as the following steps: First, strain data during free oscillation were collected by a strain gauge attached 12 mm away from the weld toe. Then, the number of cycles and magnitude of stress range in collected data were counted by using the rainflow method. Finally, the counted data were translated into the relationship between power spectra and natural frequency via the fast Fourier transform method. From the results, the natural frequency is around 26 Hz when no fatigue crack develops. It is decreased toward around 22 Hz as a fatigue crack propagates. As a result, it can be thought that the resonance does not happen if a loading frequency is less than 22 Hz. Thus, given the result, the loading frequency was chosen so that the resonance does not occur. Table 3 shows the stress ranges chosen for the pilot test under variable amplitude loading. They include low-stress ranges below 15 MPa, which is a cutoff limit given by the design code of JSSC. Loading frequencies are derived from corresponding stress ranges, and loading times are decided such that one loading sequence is approximately 9000 cycles. The mean stress is fixed to 0, and stress ratio is  $R = -1$ .

Figure 9 shows an example of stress range versus time history. The pilot test was carried out up to two loading sequences. It is observed that stress range changes automatically in the order of inputted loading sequence. To check the performance for input data, the number of cycles during one loading sequence was counted by the rainflow method. Hereafter, the number of cycles recorded from one loading

**Table 3** Detailed information of variable amplitude loading

Block number	Stress range (MPa)	Frequency (Hz)	Loading time (s)	Calculated number of cycles
1	11	12.2	175	2079
2	13	12.9	130	1720
3	15	13.5	105	1426
4	17	14.1	75	1104
5	19	14.7	60	828
6	21	15.3	40	607
7	23	15.7	30	460
8	25	16.0	21	331
9	27	16.5	14	230
10	29	16.9	9	156
11	31	17.3	5	92
12	33	17.6	4	64
13	35	17.8	2	37
14	37	18.1	2	37
15	39	18.4	1	28
Total			676	9200

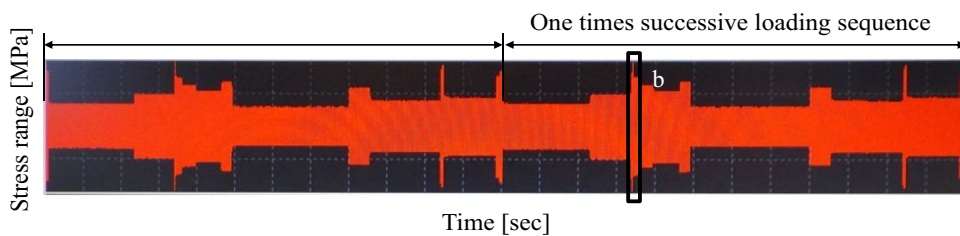
sequence is called output data, and the number of cycles calculated from one loading sequence according to frequency distribution shown in Fig. 6 is called input data. Figure 10 shows comparison of the ratio of output data versus input data. From the result, the number of cycles in the low-stress range agrees with input data at around 100%, while that of block number 15 is 30% less than input data. It can be obviously seen that the ratio of the high-stress range is lower than that of the low-stress range. To reveal the reason for this, a sequence around block number 15 is extracted and examined. Figure 9b shows a successive loading sequence of block numbers 5, 10, and 15. From the figure, one can observe that it takes time slightly to transfer loading frequency to that of the next block. This is because the loading frequency is switched in accordance with on–off timer of the ladder program. Hence, the time during the change of loading frequency needs to be considered to improve the accuracy of the system.

**4.1.3 Modification of accuracy of variable amplitude stress fatigue test**

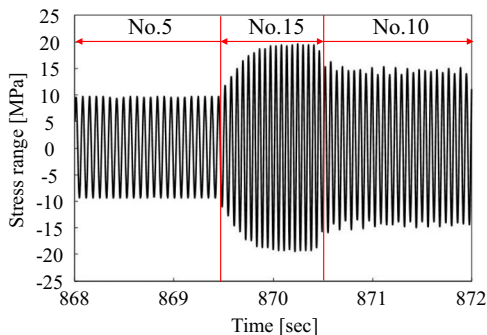
In order to improve accuracy of variable amplitude stress fatigue test, some modifications on loading time and frequency were made for the highest stress ranges, i.e., block number 15.

To increase the amount of output data of block number 15, loading time to be assigned is modified from 1.0 to 2.0, 3.0, and 4.0 s. Figure 11 shows the results of changed loading time. Because these loading sequences were taken from

**Fig. 9** Example of stress range versus time history



**a** Stress range versus time history



**b** Block number 5, 15 and 10

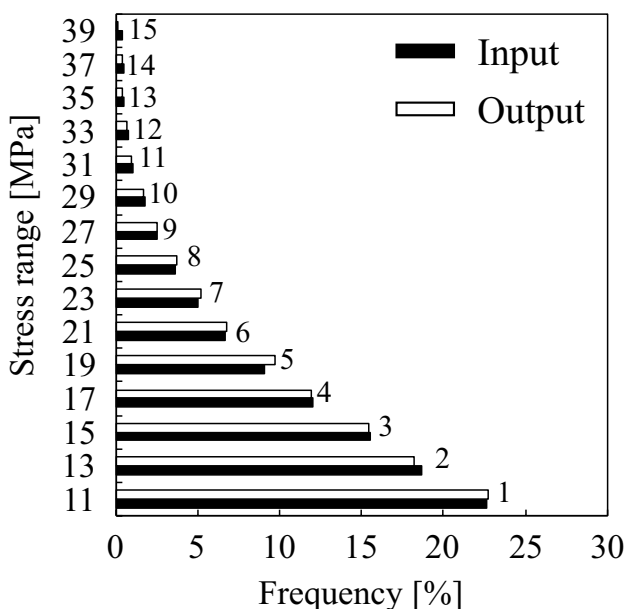


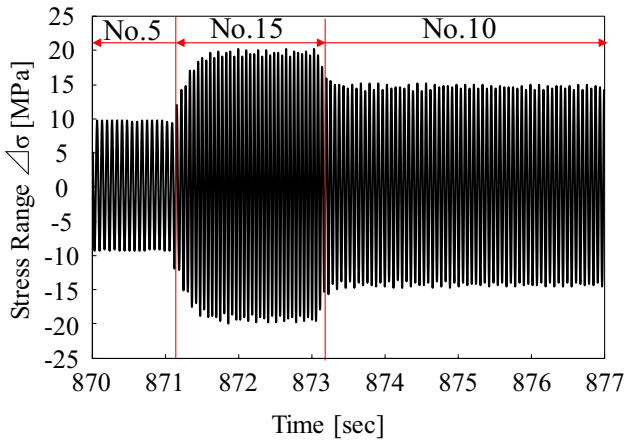
**Fig. 10** Comparison of the ratio of output data versus input data

a different pilot test, extracted time was slightly different. As an outcome, loading length of block number 15 becomes clearly longer as the loading time increases. Figure 12 shows the ratio of output data versus input data. The ratio is around 30% in 1.0 s of the loading time. The low accuracy is fairly improved up to around 90% when the loading time is set to 2.0 s. The ratio in more than 3.0 s is too high, such as 150% (in 3.0 s) and 210% (in 4.0 s). Therefore, it can be said that slight modification with respect to loading time leads to

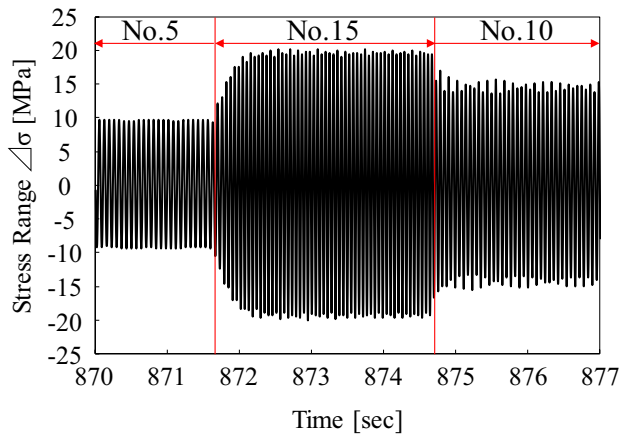
improvement of output variable stress. In subsequent tests, 2.0 s that fits the best input data was used for the loading time of block number 15.

To examine whether the order of loading sequence affects the ratio of output data versus input data of block number 15, additional pilot tests were carried out based on 13 different loading sequences. Detailed information of loading sequences is described in the authors' previous study [21]. As a result, it was found that the accuracy is decreased when the low-stress range is arranged before block number 15. Figure 13 shows a loading sequence with the low accuracy of block number 15. In this case, block number 2, whose magnitude of stress range is 13 MPa, is arranged before block number 15. Figure 12 shows the ratio of output of variable amplitude stress. It can be confirmed that the ratio of block number 15 is around 70%. Figure 14 shows the power spectrum of block number 15 along with natural frequency of out-of-plane gusset welded joint specimen shown in Fig. 8. From the result, the power spectrum of block number 15 contains natural frequency of specimen (see around 26 Hz in Fig. 14). This might be caused by loading frequencies assigned to block numbers 2 and 15. Thus, loading frequency of block number 15 was slightly adjusted from 18.4 to 18.6 Hz. The results before and after adjusted loading frequency of block number 15 are compared both in Fig. 12 and Fig. 14. From Fig. 14, the power spectrum around natural frequency is not confirmed after adjusted loading frequency. In line with the change of power spectrum, the ratio is also improved from 65 to 100%, as presented in Fig. 12. Therefore, it can be said that slight modification of applied loading frequency leads to improvement of applied stress range.

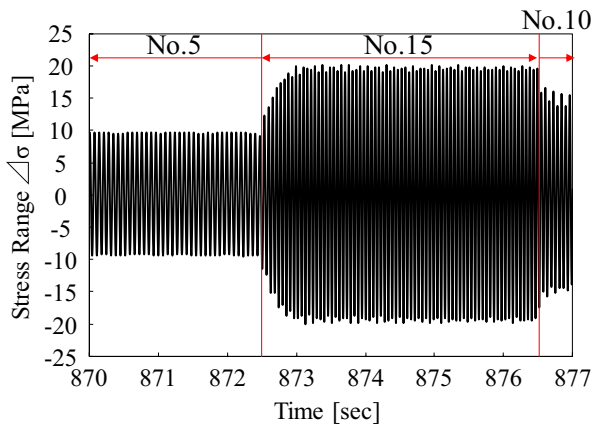




**a 2.0 sec**



**b 3.0 sec**



**c 4.0 sec**

Fig. 11 Results of changed loading time of block number 15

## 4.2 Fatigue test

### 4.2.1 Test condition

Variable amplitude stress fatigue tests were carried out using

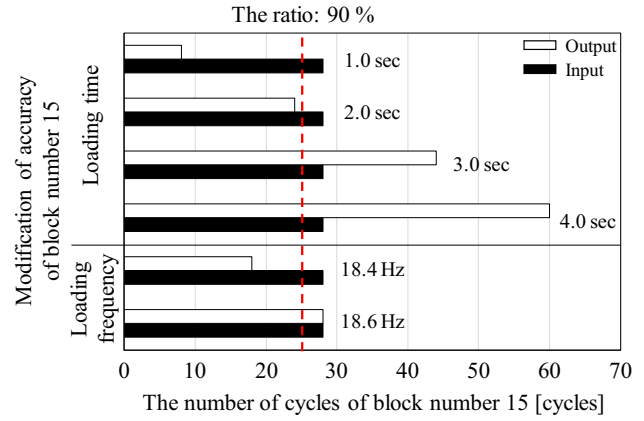


Fig. 12 The ratio of output data versus input data

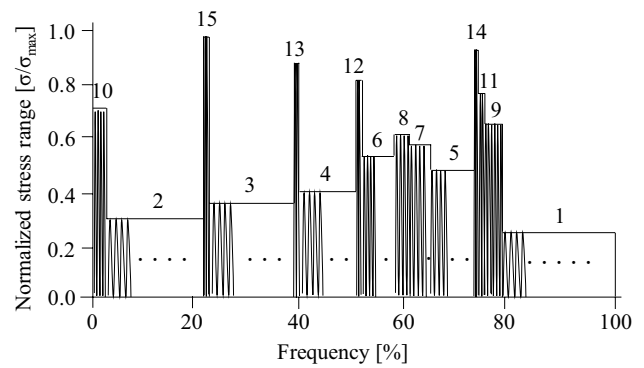


Fig. 13 Loading sequence with the low accuracy of block number 15

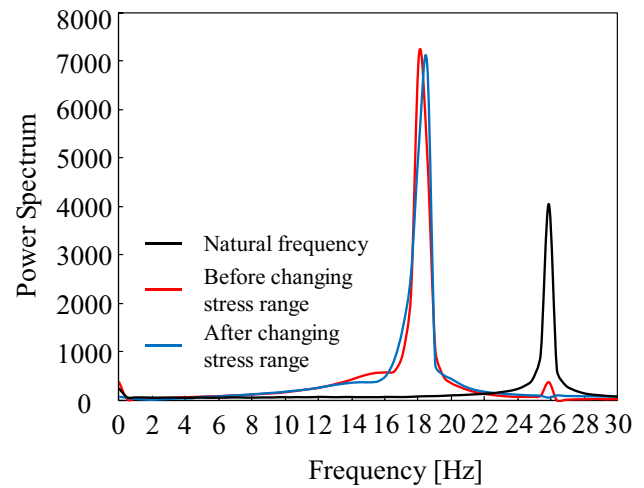


Fig. 14 Relationship between power spectrum and frequency

the developed system. The modified frequency distribution and 15-block loading sequence were utilized to the tests; see Fig. 6 and Fig. 7. Table 4 shows the list of specimens for variable amplitude stress fatigue test. A total of 12 specimens,

**Table 4** List of specimens for variable amplitude stress fatigue test and test results

Steel	Specimen	Stress ratio	Equivalent stress range (MPa)		Maximum stress range (MPa)	Minimum stress range (MPa)	Number of cycles required for reaching each fatigue life				Nc (%)	Np (%)	Damage accumulation		Crack initiation
			With cutoff	Without cutoff			N <sub>toe</sub>	N <sub>b</sub>	N <sub>10</sub>	N <sub>20</sub>			With cutoff	Without cutoff	
SM490A	VA1	-1	120	120	254	72	107,000	165,200	300,200	354,100	0.30	0.70	1.12		Weld toe
	VA2		119	119	254	72	138,000	240,300	399,600	465,000	0.30	0.70	1.47		Weld toe
	VA3		81	811	175	48	157,000	470,700	760,400	961,700	0.16	0.84	0.92		Weld toe
	VA4		81	81	171	48	295,700	596,800	963,000	1,134,900	0.26	0.74	1.08		Weld toe
	VA5		52	52	113	32	1,121,400	2,843,400	4,092,400	4,871,500	0.23	0.77	1.63		Weld toe
	VA6		48	48	102	29	1,603,900	4,079,200	5,918,400	6,881,700	0.23	0.77	1.42		Weld toe
	VA7		43	44	91	26	2,878,500	4,961,800	7,430,200	9,369,200	0.31	0.69	1.37		Weld toe
	VA8		37	37	79	22	5,717,200	8,632,300	11,891,100	13,960,600	0.41	0.59	1.31		Weld toe
	VA9		32	32	68	19	3,456,400	9,850,400	13,092,800	16,054,300	0.22	0.78	0.94	0.98	Weld toe
	VA10		26	26	58	16	23,346,300	40,312,200	48,112,000	53,750,700	0.43	0.57	1.81	2.03	Weld toe
	VA11		25	24	50	14	-	12,800,000	26,428,200	36,351,900	-	-	0.68	0.85	Weld toe
	VA12		22	18	39	11	> 500,000,000	-	-	-	-	-	-	-	Weld toe

named using the initial letters of variable amplitude loading and numbered, e.g., VA1, were tested under stress ratio of  $R = -1$ . For VA1 to VA4 specimens, they were tested to verify applicability of variable amplitude stress fatigue test using the developed system. For VA5 to VA10 specimens, the equivalence stress ranges were gradually decreased by each 5 MPa per specimen, starting from 53 MPa of VA5. This magnitude of stress range is identical to the one of failure specimen acquired from constant amplitude stress fatigue test under  $R = -1$  in the present study (see Fig. 4). For only VA11 and VA12 specimens, stress ranges below the cutoff limit are included in their variable amplitude stress. The fatigue test was continued up to fatigue life of  $N_{20}$ , and the beach mark test was not carried out.

In previous studies [26, 27], the fatigue test results were evaluated based on Woehler lines made from results of constant amplitude stress tests and Gussner lines with the maximum stress amplitude and the number of cycles to failure. They recommend this method of presentation because the degree to which the Gussner lines exceed the Woehler lines can be evaluated by the exceedance factor and the factor offers a potential for lightweight design [27]. On the other hand, the calculation of equivalent stress range was proposed [1, 2]. With this way, the variable amplitude results can be well correlated with constant amplitude ones. This study considers the equivalent stress range when arranging the fatigue test results. The equivalent stress range can be calculated on the basis of the modified Miner's rule and with the cutoff limit according to the design code of JSSC. The former rule counts all stress ranges as they affect fatigue damage. The latter rule does not count stress ranges below the cutoff limit, which is 15 MPa given by the JSSC. The equivalent stress range and damage accumulation can be formulated as the following Eqs. (2) and (3).

$$\Delta\sigma_{eq} = \sqrt[m]{\sum \frac{n_i \sigma_i^m}{N}} \tag{2}$$

$$D = \sum \left( \frac{n_i}{N} \right) \tag{3}$$

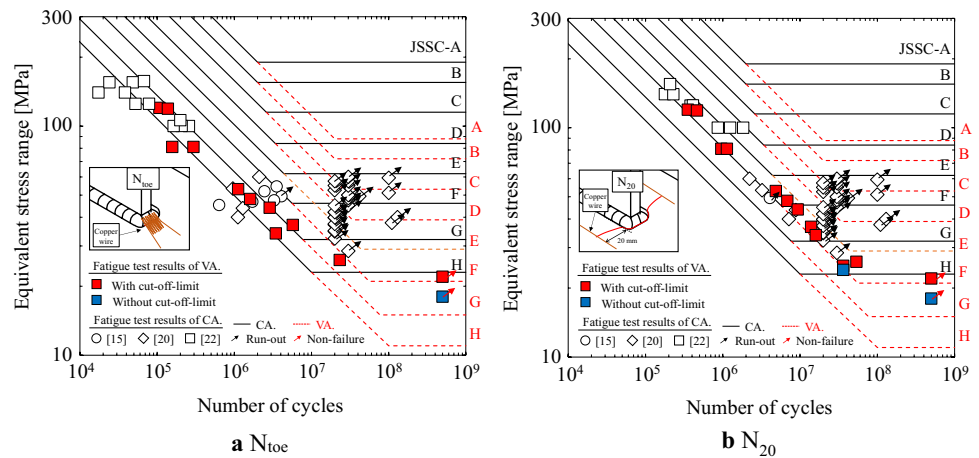
where,

- $\sigma_i$   $i$ th stress range.
- $n_i$  The number of cycles for  $i$ th stress range.
- $N$  Total of the number of cycles.
- $m$  Slope of S–N curves, and  $m = 3$  is utilized.

#### 4.2.2 Test results

Figure 15 shows the fatigue test results under variable amplitude loading, and the detailed information such as equivalent stress range and number of cycles required for reaching each

**Fig. 15** Fatigue test results under variable amplitude loading



fatigue life on fatigue crack lengths are given in Table 4. In addition, fatigue test results under constant amplitude loading in previous studies [15, 20, 22] are plotted in Fig. 15. Also indicated in this figure are the fatigue design curves for variable amplitude stress given by JSSC. The red-colored arrow mark means there is no fatigue crack initiation.

From Fig. 15a, the fatigue cracks on  $N_{toe}$  are observed at equivalent stress ranges from 25 to 120 MPa. From the results for VA1 to VA4 specimen, the fatigue strengths of  $N_{toe}$  show around JSSC-G and H class. These results are well in agreement with the constant amplitude stress fatigue test results obtained in [22]. Hence, it can be said that applicability of variable amplitude stress test using the developed system is verified. From the results for VA5 to VA6 specimens, fatigue crack initiation results because the magnitude of equivalent stress ranges is slightly larger than the CAFL, i.e., around 45 MPa based on the experimental results. On the one hand, as shown in the results for VA7 to VA11 specimens, even when the magnitude is below the CAFL, fatigue cracks are initiated. Especially for VA11 specimen, the equivalent stress range is 25 MPa, i.e., a large portion of variable amplitude stress consists of smaller stress ranges than the CAFL. In terms of the given maximum stress range for VA11, the magnitude is 50 MPa. It is found that the magnitude is larger than the CAFL; and thus, it can be said that the stress ranges larger than the CAFL contribute to fatigue crack initiation. According to a previous study [5], if any of stress range cycles contained in variable amplitude stress exceeds the CAFL, crack initiation will likely occur, even if the number of exceeded cycles is as few as one per a thousand cycles. On the other hand, in the VA12 specimen tested at 22 MPa, the fatigue crack is not confirmed even after 500 million cycles. The given maximum stress range for VA12 is 39 MPa; in other words, none of the stress range cycles contained in variable amplitude stress exceeds the CAFL. This is the reason why fatigue crack does not occur even after 500 million cycles. Although this specimen seems

not to fail, variable amplitude stress fatigue test continues. Thus, fatigue crack initiation was observed, in the case any of the stress range exceeds the CAFL, despite the equivalent stress range is below the limit. In contrast, in the case none of the stress range exceeds the CAFL, fatigue crack would not occur.

The non-failure VA12 specimen allows checking the ratio with respect to the numbers of cycles up to 500 million cycles as shown in Fig. 16. The check is respectively performed using the one loading sequence of the time when the total number of cycles reaches 50, 100, 200, 300, 400, and 500 million cycles. From the figure, especially for the ratio of the number block 15, it is confirmed that the ratio is around 90% when the total number of cycles is 50 million cycles. Furthermore, it is kept when the total number of cycles reaches until 500 million cycles. Thus, it can be said that stable variable amplitude fatigue test can be carried out using the developed system.

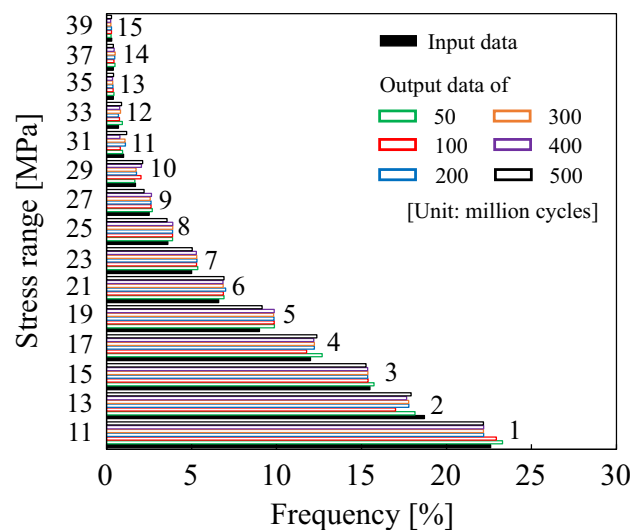


**Fig. 16** The ratio of input data to output data in the long life region

From Fig. 15b, the variable amplitude stress fatigue test results on  $N_{20}$  agree well with the constant amplitude ones and follow the curve of the modified Miner's rule. Focused on the distribution feature of data plot, the results of  $N_{20}$  fall linearly along the S–N curve. On the other hand, those of  $N_{toe}$  fall non-linearly as equivalent stress ranges get lower. Ratios of fatigue crack initiation life and fatigue crack propagation life against total fatigue life (herein,  $N_{20}$ ) are provided in Table 4. In this table, the percentages on fatigue crack initiation life ( $N_c$ ) or fatigue propagation life ( $N_p$ ) are calculated by dividing  $N_{toe}$  by  $N_{20}$ , or dividing from  $N_{toe}$  to  $N_{20}$  by  $N_{20}$ , respectively. For the VA11 specimen, the  $N_c$  and  $N_p$  were not calculated because of missing detection of  $N_{toe}$ . From Table 4, the  $N_c$  is around 30% and tends to be increased progressively in the long life region, while the  $N_p$  is around 70%. As a result, it is found that the fatigue life under variable amplitude loading in the long life region is dominated by  $N_p$ . Thus, it can be said that the distribution feature found for results of  $N_{toe}$ , i.e., non-linearity, vanishes with fatigue crack propagating.

#### 4.2.3 Damage accumulation

To examine application of the modified Miner's rule with and without cutoff limits for variable amplitude fatigue strength in the long life region, the resulting  $D$  values are discussed. For the calculation, a cutoff limit was chosen as 21 MPa of JSSC-F class based on the fatigue test results under variable amplitude stress. The  $D$  values for each specimen are in Table 4. From the table, the results assessed by the modified Miner's rule with the cutoff limit are about  $D = 1.0 \sim 2.0$ , while being the relatively low  $D = 0.7$  for VA11 specimen. If the cutoff limit is not used for the VA11 specimen, the result shows approximately  $D = 0.9$ . As a result, the modified Miner's rule gives acceptable evaluation in comparison with the results by the rule with the cutoff limit. Thus, the modified Miner's rule could give suitable evaluation to the fatigue damage accumulation of the joints under variable amplitude loading in the long life region.

#### 4.2.4 Observation of fractured surface

To reveal crack propagation, the fractured surfaces were observed. Figure 17 shows fractured surfaces obtained from constant and variable amplitude stress fatigue test. One was treated at the stress range of 53 MPa, and the other was tested at the equivalent stress range of 48 MPa where the maximum stress range was 102 MPa and the minimum stress range was 29 MPa. From the fractured surface by constant amplitude loading, in Fig. 17a, fatigue cracks of approximately 5 mm long and 1.5 mm depth were detected at 955,200 cycles as  $N_{toe}$ . The detected crack propagated in semi-ellipse shape and reached  $N_b$ ,  $N_{10}$ , and  $N_{20}$ . The beach

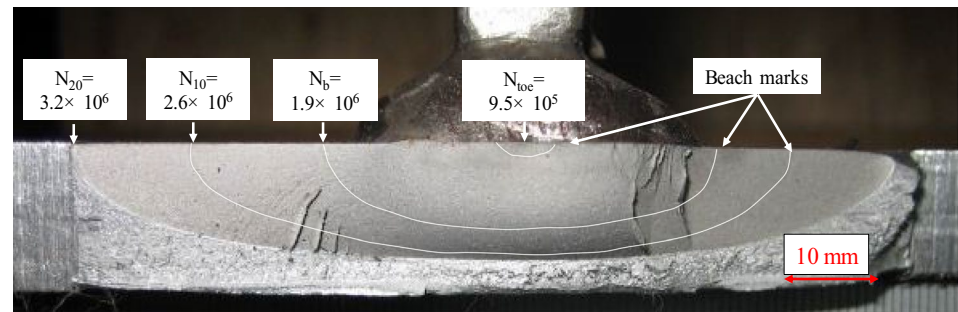
mark test was conducted at half of the stress range, around 25 MPa, when  $N_{toe}$ ,  $N_b$ , and  $N_{10}$ . As a result of the test, beach marks were clearly left on the fractured surface. On the other hand, from the fractured surface by variable amplitude loading, in Fig. 17b, although the beach mark test was not conducted during the variable amplitude stress fatigue test, plural marks having different widths are left on the fractured surface. These marks are due to fluctuation of stress range. The plural marks would be made by low stress ranges such as number block 1, 2, 3, or 4 (see Fig. 7) because a large portion of load sequence consists of these stress ranges. The marks left on the surface of around  $N_{10}$  seem to increase in comparison with the ones on the surface around  $N_{toe}$ . This implies that subjecting low-stress range became large along with fatigue crack propagation. Hence, it is found that the contribution of the low-stress range became large along with crack propagation. However, it is still unclear from surface observation when extremely lower stress ranges such as ones below the cutoff limit start to contribute to crack propagation. Thus, it can be said that the low-stress range contributes to fatigue crack propagation after fatigue crack initiation.

## 5 Conclusions

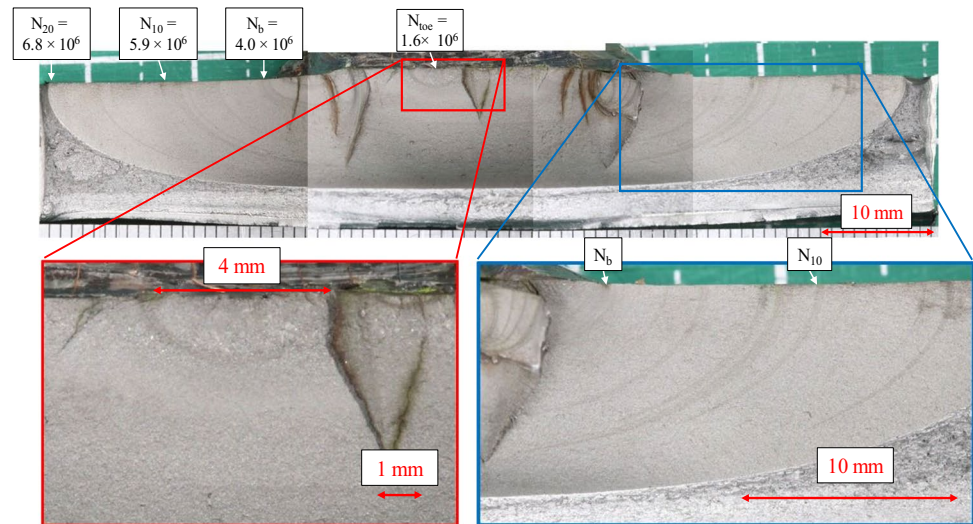
This study investigated fatigue strength of welded joints under variable amplitude plate bending loading in the long life region. Constant amplitude stress fatigue tests were conducted using a plate bending fatigue test machine in the co-authors' previous study [20] in order to obtain constant amplitude fatigue limit (CAFL). Thereafter, to carry out fatigue tests under variable amplitude stress, a loading system for the machine was originally developed, and the system's accuracy was verified in terms of a ratio of output versus input data and improved by modifying applied loading conditions. Then, variable amplitude stress fatigue tests were carried out using the developed system under several magnitudes of variable stress ranges determined based on the CAFL. The test results were discussed in terms of fatigue strength, fatigue life, and damage accumulation. The main conclusions are summarized in the following bullets:

1. From constant amplitude stress fatigue test results, the CAFL was assumed from the minimum stress range in which fatigue failure occurred and was approximately 51 MPa at  $R = 0.0$ , 40 MPa at around  $R = 0.5$ , and 45 MPa at  $R = -1$ , which tended to depend on the stress ratio.
2. By incorporating a sequencer with a ladder program into the plate bending fatigue test machine, a variable amplitude loading system was originally developed, and the system's accuracy was verified in terms of a ratio of out-

**Fig. 17** Fractured surface of constant and variable amplitude stress fatigue tests



**a** Constant amplitude loading (Fractured surface of CA11)



**b** Variable amplitude loading (Fractured surface of VA6)

put versus input data. The result shows that the accuracy can be improved up to around 90% by slightly modifying applied loading conditions. Furthermore, from the check of the accuracy after variable amplitude stress fatigue test starts, the accuracy can be maintained even when a fatigue test continues over 500 million cycles.

- From variable amplitude stress fatigue test results using the developed system and observation of fracture surface, fatigue crack initiation and propagation in the long life region were observed, in the case any of the stress components contained in variable amplitude stress exceeds the CAFL, despite the equivalent stress range being lower than it. In contrast, fatigue crack initiation was not observed until 500 million cycles when none of the stress components exceeds the CAFL.
- The application of the modified Miner's rule could provide suitable evaluation to fatigue strength of out-of-plane gusset welded joints under variable amplitude stress in the long life region when any of the stress components contained in the variable stress exceeds the CAFL.

Variable amplitude block loading fatigue tests were performed under limited conditions, such as frequency distribution and loading sequence. As used in the frequency distribution in this study, the low stress ranges below 25% of the maximum stress range are omitted. These low stress ranges could influence fatigue strength on fatigue crack propagation stage. Meanwhile, as observed on block loading test using aluminum alloys in the previous study [28], fatigue crack growth retardation and/or acceleration was observed when the order of high-low or low-high block loading sequence is used; and hence, loading sequence could also influence the fatigue strength. Thus, further comprehensive variable amplitude block loading fatigue tests are desirable using a wider frequency distribution and/or different loading sequence.

**Acknowledgements** We would like to thank Professor Kengo Anami at Shibaura Institute of Technology for providing constant amplitude fatigue test data. We would also like to acknowledge Specially Appointed Assistant Professor Yuki Ono at Gifu University for helping edit the manuscript.

## Declarations

**Conflict of interest** The authors declare no competing interests.

## References

1. Yamada K, Albrecht P (1976) Fatigue design of welded bridge details for service stress. *Transp Res Rec* 607:25–30
2. Albrecht P, Yamada K (1979) Simulation of service fatigue loads for short-span highway bridges. *Am Soc Test Mater ASTM STP* 671:255–277
3. Yamada K, Shigetomi H (1989) Constant amplitude fatigue tests in the long life region and fracture mechanics analysis. *J Struct Eng* 35A:961–968 (In Japanese)
4. Yamada K (1990) Measurement of service stress and fatigue life evaluation of bridges, IABSE Colloquium, pp.119–128
5. Fisher JW, Mertz DR, Zhong A (1983) Steel bridge members under variable amplitude, long life fatigue loading, National Cooperation Highway Research Program Bridge Reports 267. Transportation Research Board, Washington, D.C.
6. Miki C, Murakoshi J, Toyoda Y, Sakano M (1989) Long life fatigue behavior of fillet welded joints under computer simulated highway and railroad loading. *Structural Eng/Earthquake Eng* 6(1):41–48
7. Albrecht P, Lenwari A (2009) Variable-amplitude fatigue strength of structural steel bridge details: review and simplified model. *J Bridg Eng* 14(4):226–237
8. Yamada K (1985) Fatigue crack growth rates of structural steels under constant and variable amplitude block loading. *Structural Eng/Earthquake Eng* 2(2):271s–279s
9. Miki C, Sakano M, Murakoshi J (1988) A parametric study on fatigue design curves for steel highway bridges. *Structural Eng/Earthquake Eng* 5(2):235s–243s
10. Miki C, Sakano M (1990) Fatigue crack propagation analysis on fatigue design curves. *J Struct Eng* 36A:409–416 (In Japanese)
11. Mori T, Hayashi N (1996) Proposal of fatigue life evaluation method for steel structural details under variable amplitude stresses. *Journal of JSCE* 537(I–35):107–117 (In Japanese)
12. Japanese Society of Steel Construction (2012) Fatigue design recommendation for steel structures. *Gihodo*. (In Japanese)
13. EN 1993 1–9 (2005) Eurocode 3: Design of steel structures: Part 1–9: Fatigue, European committee for standardization (CEN)
14. Hobbacher FA (2016) Recommendations for fatigue design of welded joints and components, 2nd edn. Springer International Publishing, Cham, IIW document
15. Yamada K, Ya S, Baik B, Torii A, Ojio T, Yamada S (2007) Development of a new fatigue machine and some fatigue tests for plate bending. *International Institute of Welding, IIW Document XIII-2161–07*
16. Baik B, Yamada K, Ishikawa T (2008) Fatigue strength of fillet welded joint subjected to plate bending. *Steel structures* 8:163–169
17. Yamada K, Kakiichi T, Ishikawa T (2009) Extending fatigue life of cracked welded joint by impact crack closure retrofit treatment, *International Institute of Welding, IIW Document XIII-2289r1–09*
18. Yamada K, Ishikawa T, Kakiichi T, Murai K, Yamada S (2009) Fatigue test of various welded joints in plate bending. *International Institute of Welding, IIW Document XIII-2290r1–09*
19. Yamada K, Ojio T, Torii A, Baik B, Sasaki Y, Yamada S (2008) Influence of shot blasting on fatigue strength of out-of-plane gusseted specimens under bending. *J Struct Eng* 54A:522–529 (In Japanese)
20. Kinoshita K, Anami K (2013) Experimental investigation of long-life fatigue strength of out-of-plane gusset welded joints. *Proc Constr Steel* 21:814–818 (In Japanese)
21. Kinoshita K, Banno Y (2018) Development of variable amplitude loading system for plate bending fatigue test machine. *Proceeding of Construction Steel* 26:796–803 (In Japanese)
22. Japanese Society of Steel Construction (2018) JSSC technical report No.115. (In Japanese)
23. Kinoshita K, Ono Y, Banno Y, Yamada S, Handa M (2020) Application of shot peening for welded joints of existing steel bridges. *Welding in the world* 64:647–660
24. Kinoshita K, Arakawa S (2013) Fatigue crack propagation analysis considering crack aspect ratio for out-of-plane gusset joints under bending. *Structural Eng/Earthquake Eng* 69(1):20–25 (In Japanese)
25. Albrecht P, Friedland IM (1979) Fatigue-limit effect on variable-amplitude fatigue of stiffeners. *J Struct Div ASCE* 105(ST12):2657–2675
26. Sonsino MC (2007) Fatigue testing under variable amplitude loading. *Int J Fatigue* 29:1080–1089
27. Yildirim CH, Marquis G, Sonsino MC (2015) Lightweight potential of welded high-strength steel joints from S700 under constant and variable amplitude loading by high-frequency mechanical impact (HFMI) treatment. *Procedia Eng* 101:467–475
28. Borrego LP, Ferreira JM, Costa JM (2008) Partial crack closure under block loading. *Int J Fatigue* 30:1787–1796

**Publisher's Note** Springer Nature remains neutral with regard to jurisdictional claims in published maps and institutional affiliations.